analytical chemistry

pubs.acs.org/ac Article

In Situ Formation of Gold Nanoparticles Decorated Ti_3C_2 MXenes Nanoprobe for Highly Sensitive Electrogenerated Chemiluminescence Detection of Exosomes and Their Surface Proteins

Huixin Zhang, Zonghua Wang,* Feng Wang, Yimeng Zhang, Hongye Wang, and Yang Liu*

Cite This: *Anal. Chem.* 2020, 92, 5546−5553 Read Online

ACCESS | Metrics & More | Article Recommendations | Supporting Information

ABSTRACT: In this work, an ultrasensitive electrogenerated chemiluminescence (ECL) biosensor for exosomes and their surface proteins was developed by the in situ formation of gold nanoparticles (AuNPs) decorated Ti_3C_2 MXenes hybrid with aptamer modification (AuNPs-MXenes-Apt). In this strategy, the exosomes were efficiently captured on an exosome recognized CD63 aptamer modified electrode interface. Meanwhile, in situ formation of gold nanoparticles on single layer Ti_3C_2MXenes with aptamer (MXenes-Apt) modification was obtained, in which MXenes acted as both reductants and stabilizer, and no additional reductant and stabilizer involved. The in situ formed AuNPs-MXenes-Apt hybrid not only presented highly efficient recognition of exosomes specifically, but also provide naked catalytic surface with high electrocatalytic activity of gold nanoparticles with predominated (111) facets that significantly improved the ECL signal of luminol. In this way, a highly sensitive ECL biosensor for exosomes detection was constructed ascribing to the synergistic effects of large surface area, excellent conductivity, and catalytic effects of the AuNPs-MXenes-Apt. The detection limit is 30 particles μL^{-1} for exosomes derived from HeLa cell line, which was over 1000 times lower than that of conventional ELISA method and the linear range was from 10^2 particles μL^{-1} to 10^5 particles μL^{-1}. This ECL sensing platform possessed high selectivity toward exosomes and their surface proteins derived different kinds of tumor cell lines (HeLa cells, OVCAR cells and HepG2 cells), and enabled sensitive and accurate detection of exosomes from human serum, which implied that the ECL biosensor provided a feasible, sensitive, and reliable tool for exosomes detection in exosomes-related clinical diagnostic.

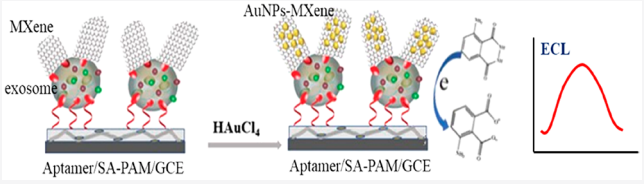

INTRODUCTION

Exosomes are secreted by multiple cells,[1] including B cells, T cells, dendritic cells, macrophages, tumor cell lines and stem cells, vesicles with a diameter of 30−200 nm. Because of their diverse sources, they have an ability to carry abundant biomolecule, such as lipids, proteins, RNA, DNA, and other biological molecules.[2−4] At present, more and more evidence indicated that exosomes have a lot to do with the disease, could be ideal biomarkers for early diagnosis.[5,6] An effective method for exosomes and their surface proteins detection is crucial in the diagnosis and therapies of diseases. Currently, exosomes detection mostly relies on dynamic light scattering (DLS), nanoparticle tracking (NTA), fluorescence, electrochemical method, ELISA, and so on.[7,8] In particular, electrochemical methods have become popular for exosomes detection owing to the high sensitivity, low price, and facility. For example, the catalytic molecule machine amplified method and the muli-leg exogenous walker induced a cascade-amplified strategy have been developed for the electrochemical detection of exosomes.[9,10] Although these methods are efficient and accurate, it is still a challenge to develop sensitive, low cost and reliable methods for the detection of exosomes.

In recent years, electrogenerated chemiluminescence (ECL),[11−13] a light emission from a redox reaction of electrogenerated reactants, has been widely used in many fields such as immunoassay, food safety and environmental inspection, enzymes, clinical diagnosis, and so on,[14−17] due to its high sensitivity, rapidity, easy controllability, and low cost.[18,19] In order to improve the performance, various nanocomposites have been increasingly used in ECL biosensors due to their excellent electrical conductivity, large surface area, good biocompatibility, excellent catalytic properties, in which the nanomaterials can not only act as a carrier for signal molecules but also increase the interfacial electron transfer.[20,21] The ECL biosensor was also reported for exosomes detection by using nanocomposite such as g-C_3N_4 nanosheets coated Galinstan liquid metal nanohybrids,[22] black

Received: February 2, 2020
Accepted: March 18, 2020
Published: March 18, 2020

https://dx.doi.org/10.1021/acs.analchem.0c00469
Anal. Chem. 2020, 92, 5546−5553

Scheme 1. Principle of the ECL Biosensor for Exosomes Detection Based on in Situ Formation of Gold Nanoparticles Decorated Ti_3C_2 MXenes Nanoprobes

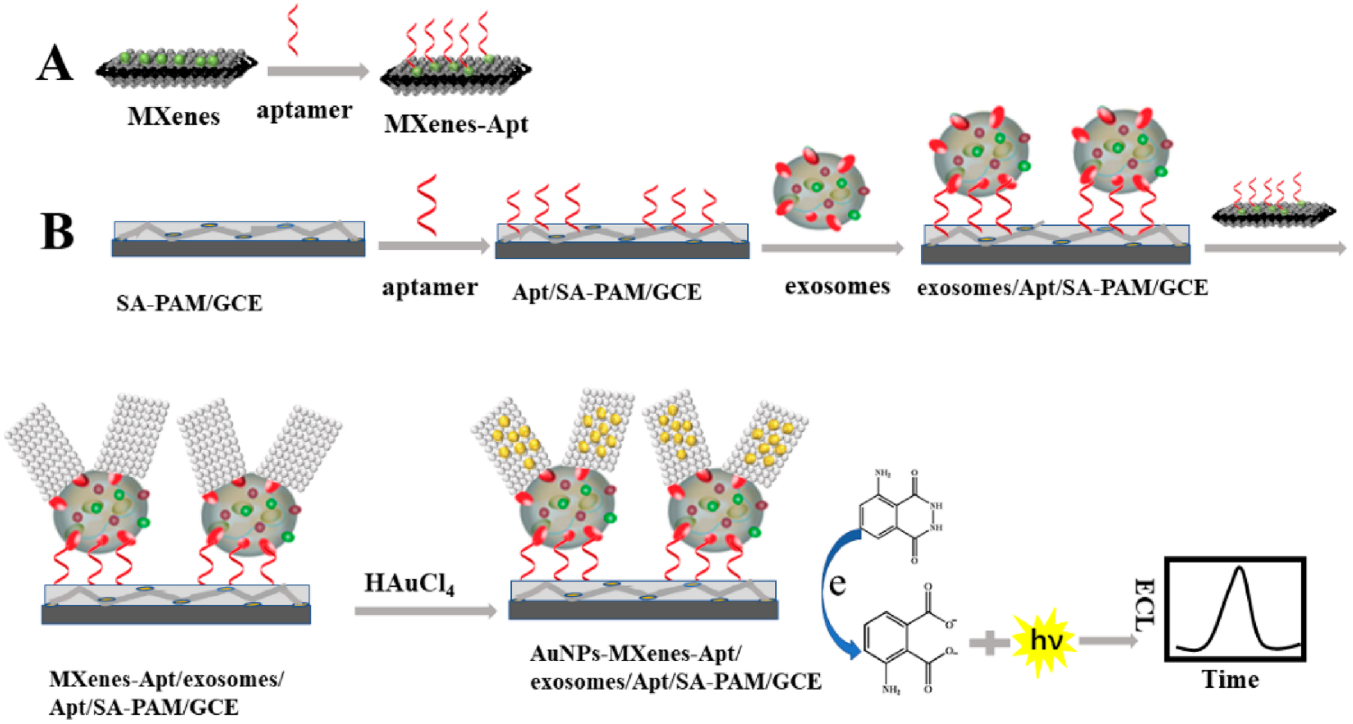

phosphorus quantum dots (QDs) modified MXenes as the signal amplifiers,[23] which obviously improved the performance. The electrocatalytic activity of nanomaterials, such as metal nanoparticles, metallic oxides, etc., are dependent strongly on the exposed facets.[24−28] In addition, the structure and morphology of the nanoparticles are crucially relied on the stabilizer ligand during the synthesis, which can avoid the aggregation of the nanoparticles. Whereas the stabilizer, such as surfactants etc., may also cover the active sites and hinder the electron transfer.[29−32] As a result, the surfactant free nanomaterials with excellent conductivity and the electrocatalytic features may provide a valuable pathway for the design of the ECL biosensor with superior performance.

Ti_3C_2 MXenes, a member of 2D layer nanomaterial, have been of wide concern.[33−35] MXenes nanosheets show special nanostructures with large surface area, and present excellent electron transfer ability, catalytic ability, good biocompatibility, and so on.[36−38] Moreover, the Ti_3C_2 MXenes also have strong reduction ability, which make them quite popular in constructing MXenes/metal nanoparticle hybrids. For example, MXenes/Ag composites and MXenes/magnetic iron oxide nanocomposites have been synthesized via the strong reducing property of MXenes, showing unusual electrocatalytic activity, catalytic ability, and so on.[39−41] The unique features of MXenes make them promising in fabrication of surfactant free nanohybrids with excellent performance for biosensing applications.

In this work, a novel ECL biosensor for highly sensitive detection of exosomes was developed by in situ decoration of AuNPs on aptamer modified MXenes (AuNPs-MXenes-Apt) as the ECL nanoprobes. In this strategy, exosomes recognized CD63 aptamer was modified on sodium alginate (SA), and poly(acrylamide) (PAM) modified the electrode. After the capture of the exosomes, the MXenes conjugated with CD63 recognized aptamer were adsorbed on the exosomes on the electrode. After the immersion in the $HAuCl_4$ solution, AuNPs decorated MXenes (AuNPs-MXenes-Apt) hybrid nanoprobes formed, in which the MXenes acted as both reductants and stabilizer to in situ produce amounts of AuNPs on their interface to form AuNPs-MXenes-Apt nanoprobes. In addition, the large surface area of MXene provide excellent conductive support to accommodate more gold nanoparticles and more recognition of active sites, and thus the AuNPs-MXenes-Apt hybrid nanoprobes can not only present highly efficient recognition of exosomes, but also provide naked catalytic surfaces with high electrocatalytic activity of AuNPs that greatly improved the ECL signal of luminol. The fabricated ECL biosensor exhibited excellent performance with the limit of detection (LOD) down 30 particles μL^{-1} ,and the linear range was over 3 orders of magnitude, which is better than those of most currently reported methods. In addition, this assay can enable sensitive and accurate detection of exosomes from human serum. Moreover, this ECL biosensor possessed high selectivity toward exosomes, and their surface proteins derived from different tumor cell lines (HeLa cells, OVCAR cells, and HepG2 cells) were also identified. The constructed ECL biosensor provided a valuable tool for the physiological functions studies of exosomes and clinic diagnostic.

■ EXPERIMENTAL SECTION

The subsection of materials, apparatus and the preparation of MXenes are described in the Supporting Information (SI).

The MXenes-glycine was synthesized as follows.[42] 0.075 mg mL^{-1} of a MXenes solution (10 mL) was added dropwise to 0.25 mg mL^{-1} glycine solution (20 mL) and stirred for 24 h. The obtained samples were freeze-dried. The XPS and FT-IR spectra were used to characterize the obtained MXenes-glycine.

https://dx.doi.org/10.1021/acs.analchem.0c00469
Anal. Chem. 2020, 92, 5546−5553

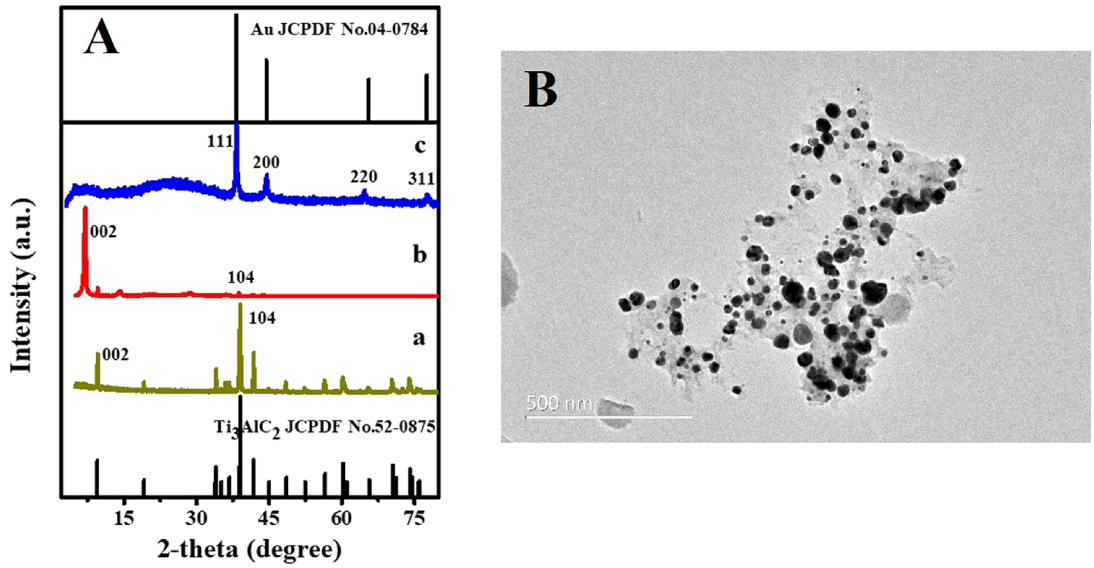

Figure 1. (A) XRD patterns of (a) Ti_3AlC_2, (b) MXenes, and (c) AuNPs-MXenes. (B) The HRTEM image of AuNPs-MXenes.

The peak at 1630 cm^{-1} in glycine (curve c) corresponded to the N−H bending vibration in glycine as shown FT-IR spectra (SI Figure S1A) The peaks at ∼3700 and ∼665 cm^{-1} (curve b) corresponded to the O−H and Ti−O tensile vibration in MXenes, respectively. The above three characteristic peaks can also be observed in curve a. These results indicated that glycine was successfully conjugated to MXenes. The interaction between MXenes and glycine was further studied by XPS, as shown in SI Figure S1B for the N-1s spectra. Despite the peak at 399.6 eV from pyrrolic C−N−H in glycine, the other peak at 397.7 eV suggested the formation of Ti−N bonds. This confirmed that the MXenes surface has been modified with glycine. The Apt (1 μM) was activated by EDC (400 mM) and NHS (100 mM) for 1 h at 37 °C. Then, 200 μL MXenes-glycine solution was added to the above solution and reacted 1 h. Finally, the sediment (MXenes-Apt) was obtained by centrifugation.

Cell Culture, Exosomes Preparation, and Characterization. Human hepatoma cells (HepG2 cells), cervical cancer cells (HeLa cells), and human ovarian cancer cells (OVCAR cells) culture, exosome production are described in detail in the SI.[43] The results showed that the size of exosomes derived from HeLa cells was about 76 nm (SI Figure S2A) and the concentration of exosomes derived from HeLa cells was approximately 1.95 × 10^8 particles mL^{-1} (SI Figure S2B).

Biosensor Fabrication. Here used bare glassy carbon electrode (GCE) was polished with 0.05 and 0.3 μm alumina powder by turns and washed with DI water and ethanol, respectively. Six μL of PAM (0.1 mg/mL) was dropped on pretreated GCE to gain PAM/GCE, 10 mg/mL (2 mL) SA was activated by the mixed solution with 2 mL EDC/NHS (100 mM/300 mM) for 1 h. Then, PAM/GCE was immersed into above solution at 37 °C for 1 h. The SA-PAM/GCE was incubated in 1 μM Apt solution at 37 °C for 2 h to finish the modification of Apt. The Apt/SA-PAM/GCE was immersed in the exosomes derived from HeLa cells certain concentrations. Finally, the exosomes/Apt/SA-PAM/GCE was incubated with MXenes-Apt for 2 h at 37 °C. Then, the MXenes-Apt/exosomes/Apt/SA-PAM/GCE was immersed in $HAuCl_4$ solution (2 mg/mL) to in situ form AuNPs (AuNPs-MXenes-Apt/exosomes/Apt/SA-PAM/GCE). Finally, the AuNPs-MXenes-Apt/exosomes/Apt/SA-PAM/GCE electrode was used for ECL detection.

RESULTS AND DISCUSSION

Fabrication of ECL Biosensor for Exosomes Detection. Scheme 1 presented the ECL biosensor for detection of exosomes GCE surface modified the SA-PAM layer provided the carboxyl group for CD63 Apt immobilization, so that more CD63 Apt molecules were modified on the electrode. After exosomes were captured, the electrode was incubated in the MXenes-Apt solution based on high specificity between Apt and CD63 protein on exosomes surface. Finally, these modified electrodes were immersed in $HAuCl_4$ solution (2 mg mL^{-1}) to form AuNPs-MXenes-Apt/exosomes/Apt/SA-PAM/GCE. The ECL signal of above electrode was record in luminol solution. Here, MXenes nanosheets can not only accommodate a large number of aptamers for highly efficient exosomes capture, but also catalyze the ECL of luminol. Moreover, the Ti_3C_2 MXenes further act as a reducing agent to in situ generate AuNPs decorated on their surface, which further amplify the ECL signals of luminol by the synergetic catalytic effect of AuNPs and MXenes that make it promising in preparation of sensitive ECL biosensor for exosomes detection.

Characterization of Ti_3C_2 MXenes and AuNPs-MXenes. The successful synthesis of Ti_3C_2 MXenes and AuNPs-MXenes were confirmed by XRD and HRTEM. Figure 1A shows the XRD pattern Ti_3AlC_2 before (a) and after LiF and HCl stripping (b). After etching, the main peak (104) disappeared, and the (002) peak of Ti_3AlC_2 shifted indicated that the bulk was stripped. The facts indicated that Ti_3C_2 MXenes were successfully prepared. As shown in Figure 1A curve c, the XRD pattern of the AuNPs-MXenes exhibited several diffraction peaks which can be indexed to diffractions from the (111), (200), (220), and (311) facets of face-centered cubic Au. More importantly, compared with the (002) peak intensity in the XRD pattern of MXenes (curve b), the (002) peak intensity in the XRD pattern of AuNPs-MXenes weakened, which can be presumed to be partial oxidation of MXenes nanosheets during the reduction reaction of AuNPs. The HRTEM image further proved the above

https://dx.doi.org/10.1021/acs.analchem.0c00469
Anal. Chem. 2020, 92, 5546−5553

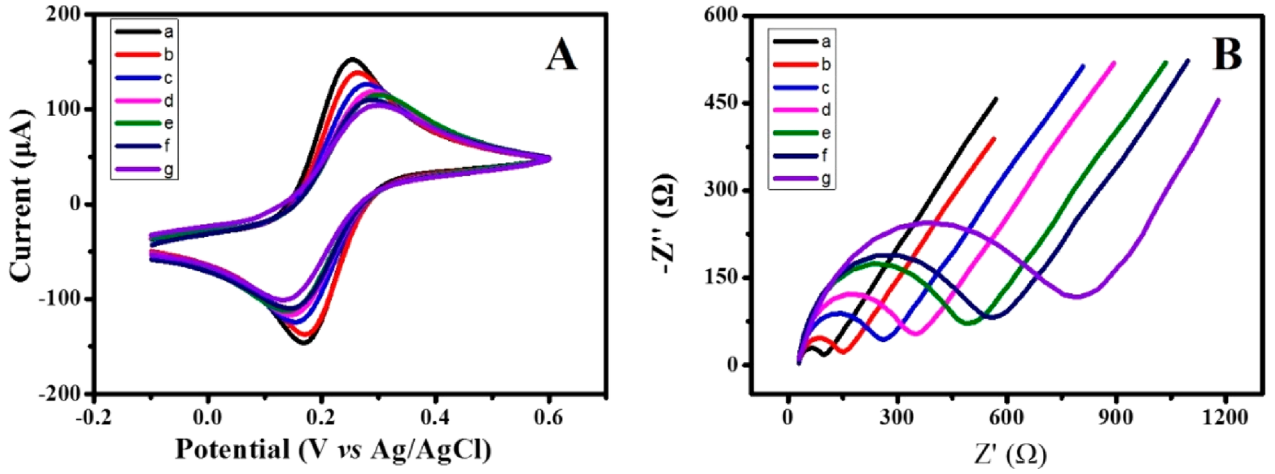

Figure 2. Cyclic voltammograms (A) and electrochemical impedance spectra (B). Bare GCE (a), PAM/GCE (b), SA-PAM/GCE (c), Apt/SA-PAM/GCE (d), exosomes/Apt/SA-PAM/GCE (e), MXenes-Apt/exosomes/Apt/SA-PAM/GCE (f), and AuNP-MXenes-Apt/exosomes/Apt/SA-PAM/GCE (g) in 5 mM $[Fe(CN)_6]^{3-/4-}$ containg 0.1 M KCl solution (pH 7.0). Scan rate was 100 mV s^{-1}. The impedance spectra were recorded from 0.1 Hz to 100 kHz with signal of 5 mV at the formal potential of the redox couple. The concentration of exosomes is 5×10^3 particles μL^{-1}.

results (Figure 1B), it can be clearly seen that AuNPs were decorated on the MXenes. The successful synthesis of MXenes was also confirmed by TEM patterns, DLS and AFM patterns (SI Figure S3). After exfoliating, monodisperse morphology can be seen, confirming the successful exfoliation of few or single layer MXenes nanosheets (SI Figure S3A). The DLS data revealed the formation of MXenes nanosheets with an average diameter about 300 nm (SI Figure S3B). The thickness of the MXenes nanosheets were characterized by AFM, which was about 1.1 nm (SI Figure S3C), indicating that MXenes were mainly single layer. To further confirm the successful synthesis of AuNPs-MXenes, the compositions of the MXenes and AuNPs-MXenes were characterized by XPS (SI Figure S4). The wide peak from 455−462 eV in SI Figure S4B implied the possible existence of low valence Ti species, such as Ti(II) at ∼455.3 eV), Ti−C bands at ∼456.2 eV and Ti−O at ∼461.5 eV. On the other hand, the formation process of AuNPs-MXenes composite can cause the transference from Ti(II) species to the Ti(IV) species (SI Figure S4C). The AuNPs-MXenes composite (SI Figure S4D) shows peaks at 83.7 and 87.3 eV, where the binding energy gap was 3.6 eV and was the characteristic of the reduced form of Au(0). These results further confirmed that AuNPs were formed on the Ti_3C_2 MXenes. The facts were also confirmed by the EDS mappings (SI Figure S5). In addition, the UV−vis absorption spectrum of Ti_3C_2MXenes nanosheets showed the typical absorption range of 750−850 nm and about 280 nm (SI Figure S6), ascribing to their interband transitions. After the addition of $HAuCl_4$ and the following reduction reaction, the absorption peak at 750−850 nm disappeared, and the peak at about 280 nm became weaker. Moreover, an absorption peak at about 550 nm occurred, attributing to the surface plasmon absorption of AuNPs. In addition, the gold nanoparticles on MXene formed quickly at room temperature, unlike those using amino acids (i.e., alanine, glycine, histidine, and lysine) and sodium alginated as the reductant that the procedures of heating or a long time were generally needed. Moreover, it was clear that the obvious oxidative peak in the cyclic voltammetry of MXene disappeared when the AuNPs MXenes formed, as a while, the oxidative peak of gold was observed at the potential over 0.9 V (SI Figure S7). These facts further confirmed the in situ decoration of gold nanoparticles on the Ti_3C_2 MXenes nanosheets owing to the excellent reductive ability.

Electrochemical Characterizations of the Assembly Processes of the Biosensor. EIS and CV were used to verify the electrode assembly processes step by step. Figure 2A shows the CV curves of the modified GCE using $Fe(CN)_6^{4-/3-}$ as electroactive probes. A clear reversible redox peek was observed in the CVs. The peak current gradually after the modification of PAM, SA and Apt, owing to the electron inert features, and it further decreased after exosomes derived from HeLa cells were captured ascribing to the specific interaction between aptamer and the CD63 protein on the exosomes. Owing to the electron inertness of Apt and exosomes, the electron and mass transfer of $Fe(CN)_6^{4-/3-}$ ions on the electrode interface were hindered. When, the exosomes/Apt/SA-PAM/GCE was modified with MXenes-Apt, the peak currents were also decreased (curve f). In addition, the MXenes-Apt/exosomes/Apt/SA-PAM/GCE was immersed with the $HAuCl_4$ solution, the peak currents were decreased obviously (curve g). Due to the negative charge of AuNPs, the mass transfer of $Fe(CN)_6^{4-/3-}$ at the electrode interface was hindered. The EIS curves are shown in Figure 2B. The Nyquist diagram includes a semicircular part in the higher frequency range in which the diameter equals the electron transfer resistance (Ret) at the electrode interface. After the electrode surface layer was assembled, the resistance was getting bigger and bigger. These results have the same trend as those of the CV, demonstrating the success of assembling biosensor.

ECL Behaviors of the Biosensor. In this work, the ECL responses from AuNPs-MXenes-Apt nanoprobes were closely related with the captured exosomes. The ECL behaviors of the biosensor were studied in the solution with 100 μM luminol (SI Figure S8). The bare GCE electrode (curve a), PAM/GCE (curve b), and Apt/SA-PAM/GCE (curve c) showed low ECL signal. In addition, exosomes/Apt/SA-PAM/GCE displayed lower ECL signals. Because electron transfer at the electrode interface was inhibited by the exosomes (curve d). A strong ECL signal can be observed only by immersing the Apt/SA-PAM/GCE with exosomes following by AuNPs-MXenes-Apt hybrid formation, as shown in (curve e). In addition, series of

https://dx.doi.org/10.1021/acs.analchem.0c00469
Anal. Chem. 2020, 92, 5546−5553

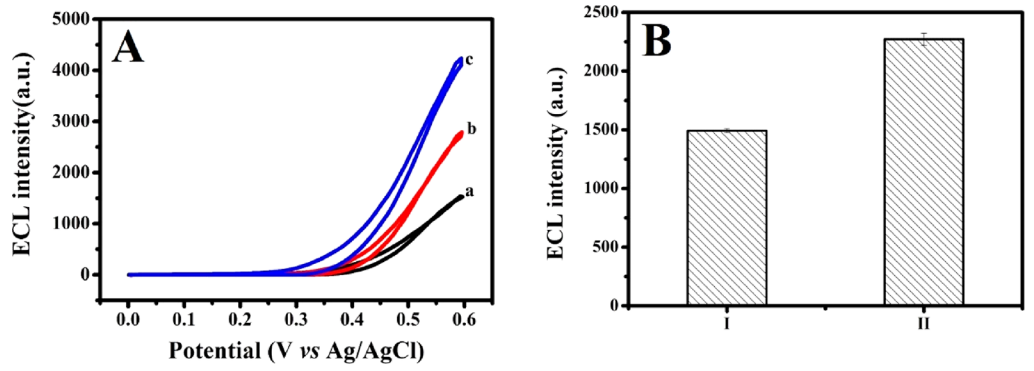

Figure 3. (A) ECL intensity of AuNPs/exosomes/Apt/SA-PAM/GCE (a), MXenes-Apt/exosomes/Apt/SA-PAM/GCE (b), and AuNPs-MXenes-Apt/exosomes/Apt/SA-PAM/GCE (c) in the solution with 100 μM luminol. The potential range of the scan was 0−0.6 V. (B) ECL intensity of the AuNPs-MXenes-Apt/exosomes/Apt/PAM/GCE (I), AuNPs-MXenes-Apt/exosomes/Apt/SA-PAM/GCE (II). The concentration of exosomes is 5×10^3 particles μL^{-1}.

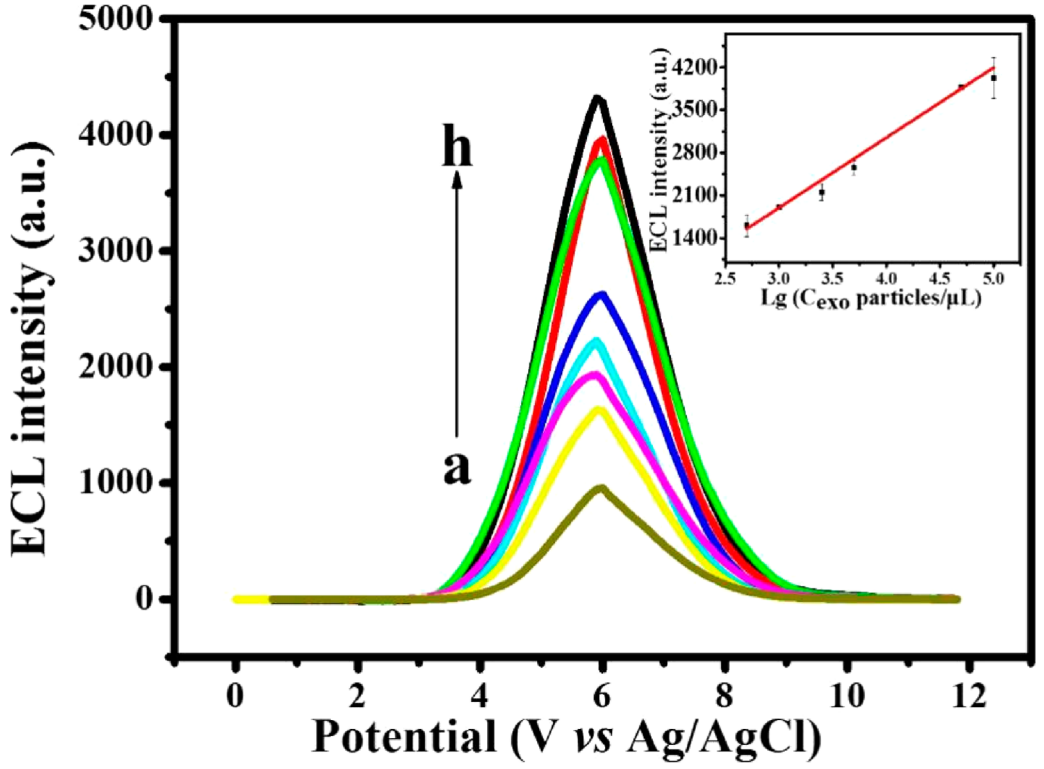

Figure 4. ECL intensities of the ECL biosensor with different exosomes concentrations (a−h: 10^2, 5×10^2, 10^3, 2.5×10^3, 5×10^3, 10^4, 5×10^4, 10^5 particles μL^{-1}) in the solution with 100 μM of luminol. The PMT voltage is 600 V.

control experiments were performed to verify feasibility of this ECL biosensor as shown in Figure 3A. The ECL responses on the AuNPs-MXenes-Apt/exosomes/Apt/SA-PAM/GCE electrodes (curve c) were obviously larger than that AuNPs/exosomes/Apt/SA-PAM/GCE electrode (curve a) and MXenes-Apt/exosomes/Apt/SA-PAM/GCE (curve b), which confirmed that the in situ formed AuNPs-MXenes-Apt hybrid not only presented highly efficient recognition of exosomes specifically, but also provide naked catalytic surface with high electrocatalytic activity of AuNPs that significantly improved the ECL signal of luminol. These results indicated that the proposed biosensor was sensitive and feasible.

In order to confirm that Sodium alginate (SA), modified the electrode surface provides more recognition sites for the aptamer, thereby improving the capture efficiency of the exosomes. As shown in Figure 3B, AuNPs-MXenes-Apt/exosomes/Apt/PAM/GCE was chosen as a control sample to fabricate a biosensor in the same conditions as that of AuNPs-MXenes-Apt/exosomes/Apt/SA-PAM/GCE. The AuNPs-MXenes-Apt/exosomes/Apt/SA-PAM/GCE (II) displayed the larger ECL signal than AuNPs-MXenes-Apt/exosomes/Apt/PAM/GCE (I). The fact could be ascribed to the more recognition sites for the conjugation of aptamer, as well as the adsorption of exosomes and AuNPs-MXenes-Apt and dramatically improved ECL signal of luminol, which could be applied for sensitive biosensor fabrication.[44]

Optimization of the Detection Conditions. Exosomes incubation temperature is important to the biosensor performances. The largest ECL signal was obtained at the temperature of 37 °C as shown in (SI Figure S9A). Another important factor for ECL sensing was the incubation time of exosomes, the optimal exosomes incubation time was 120 min in (SI

https://dx.doi.org/10.1021/acs.analchem.0c00469
Anal. Chem. 2020, 92, 5546−5553

Figure S9B). The concentration of luminol also affects the performance of this ECL biosensor. As shown in (SI Figure S9C), as the concentration of luminol increases, the ECL intensity increases and then reaches a maximum at 100 uM. Meanwhile, the ECL intensity of 1 μM Apt was largest in SI Figure S9D and the optimal concentrations of Apt of 1 μM was chosen. In addition, the incubation time of MXene in $HAuCl_4$ solution was also optimized to study the formation of gold nanoparticles/MXene on the effect toward the ECL response. It was found that the maximal ECL response was obtained when the immersion time was 120 min with the concentration of $HAuCl_4$ was 2 mg mL^{-1}, and the response nearly kept stable (SI Figure. S10). As a result, the optimal incubation time of 120 min was used in the following experiments.

The Sensitivity of the ECL Biosensor. Under the optimum conditions, the detection of the exosomes derived from HeLa cells were performed by the designed ECL biosensor. Figure 4 indicated the ECL signal intensities of luminol of the biosensor in the solution with different concentrations exosomes derived from HeLa cells. It was shown that the ECL intensities increased as the exosomes concentration increases, and it was linear with the logarithm of the exosomes concentration in the range from 10^2 to 10^5 particles μL^{-1}. The detection limit (3σ) was calculated to be 30 particles μL^{-1}(S/N = 3) with a correlation coefficient of R^2 = 0.9962, which was lower than conventional ELISA method and were reported.[45] The high sensitivity of the biosensor could be attributed to the catalysis of AuNPs-MXenes-Apt nanoprobes toward luminol ECL reaction that improved the ECL signal significantly. This fact indicated that the proposed ECL biosensor was facilitated to determine exosomes quantitatively. The reproducibility of the biosensor was also verified. The relative standard deviation (RSD) can be proved the reproducibility of ECL biosensor. These results showed that the RSDs of ECL biosensors with exosomes concentrations of 5×10^4 particles μL^{-1} and 10^4 particles μL^{-1} were 1.24% and 2.1%, respectively. indicting the good reproducibility of this ECL biosensor. In addition, the ECL response of the continuous scan of the biosensor is shown in (SI Figure S11). A stable ECL signal was obtained, suggesting that the ECL biosensor for exosomes detection possess good stability.

Detection of Exosomes in Real Sample and the Surface Proteins on Exosomes Derived from Different Cell Lines. To prove the clinical utility of this ECL biosensor, different concentrations of exosomes derived from HeLa cell were added to the serum and gain the ECL responses. The recoveries were obtained ranged from 98% to 104% in (SI Table S1). The above results demonstrated that ECL biosensor based on the AuNPs-MXenes-Apt nanoprobes could be used for the detection of exosomes in serum. The applicability was a critical issue for this fabricated ECL biosensor.

The proteins on the surface of exosomes play an important role in immune response, cell migration, cell differentiation, tumor invasion. In this strategy, ECL intensity was not only related to the concentration of exosomes, but also associated with the level of CD63 protein expressed on the surface of exosomes. Therefore, the fabricated biosensor can be used for detecting the surface CD63 proteins derived from different exosomes. As shown in Figure 5, the largest ECL signal was obtained the exosomes derived from HeLa cells. The smallest ECL signal was obtained in exosomes solution derived from the OVCAR cells. The results indicated the expression level of CD63 on the exosomes derived from HeLa cells was the highest, while the expression of CD63 on the exosomes derived from OVCAR is low, which was similar to those reported.[46] The facts demonstrate that the as designed ECL biosensor can be used to evaluate the proteins expression on exosomes, which are promising for clinical diagnosis and the prognosis of disease.

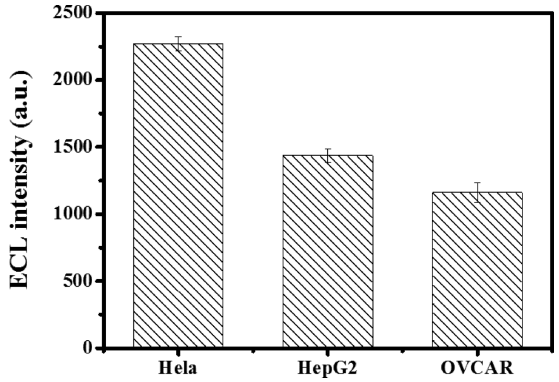

Figure 5. ECL intensity of the biosensor toward the exosomes at a concentration of 5×10^3 particles μL^{-1} derived from different cell lines.

CONCLUSIONS

In summary, a highly sensitive ECL biosensor based on the CD63 aptamer-modified SA-PAM electrode interface using the in situ formed AuNPs-MXenes-Apt nanoprobe for highly sensitive detection of exosomes were developed. The exosomes were highly efficient captured on a SA-PAM electrode interface. In addition, the in situ formed AuNPs-MXenes-Apt hybrid not only presented highly efficient recognition of exosomes specifically, but also provided naked catalytic surface with high electrocatalytic activity of gold nanoparticles with predominated (111) facets that significantly improved the ECL signal of luminol. Owing to the synergetic catalytic effect of the AuNPs-MXenes on the ECL reaction of luminol, sensitive detection of exosomes with a limit of detection as low as 30 particles μL^{-1} was obtained. The as prepared ECL biosensor can also be applied for the detection of exosomes secreted by different cancer cells in serum, indicating that the ECL biosensor is promising in clinical exosomes detection and biomedical studies.

ASSOCIATED CONTENT

Supporting Information

The Supporting Information is available free of charge at https://pubs.acs.org/doi/10.1021/acs.analchem.0c00469.

Materials and reagents, apparatus and characterization, the preparation of Ti_3C_2 MXenes, cell culture, exosomes extraction and characterization, MXenes-glycine characterizations, MXenes and AuNPs-MXenes characterization, biosensor characterization, biosensor conditions optimization and the exosomes activity analysis in serum using the biosensor (PDF)

AUTHOR INFORMATION

Corresponding Authors

Zonghua Wang − *Shandong Sino-Japanese Center for Collaborative Research of Carbon Nanomaterials, College of Chemistry and Chemical Engineering, Qingdao University,*

https://dx.doi.org/10.1021/acs.analchem.0c00469
Anal. Chem. 2020, 92, 5546−5553

Qingdao, Shandong 266071, China; orcid.org/0000-0002-9120-4089; Phone: 86-532-85950873; Email: wangzonghua@qdu.edu.cn; Fax: 86-10-62771149

Yang Liu − *Department of Chemistry, Beijing Key Laboratory for Analytical Methods and Instrumentation, Kay Lab of Bioorganic Phosphorus Chemistry and Chemical Biology of Ministry of Education, Tsinghua University, Beijing 100084, China;* orcid.org/0000-0003-0042-5183; Email: liu-yang@mail.tsinghua.edu.cn

Authors

Huixin Zhang − *Department of Chemistry, Beijing Key Laboratory for Analytical Methods and Instrumentation, Kay Lab of Bioorganic Phosphorus Chemistry and Chemical Biology of Ministry of Education, Tsinghua University, Beijing 100084, China; Shandong Sino-Japanese Center for Collaborative Research of Carbon Nanomaterials, College of Chemistry and Chemical Engineering, Qingdao University, Qingdao, Shandong 266071, China*

Feng Wang − *Department of Chemistry, Beijing Key Laboratory for Analytical Methods and Instrumentation, Kay Lab of Bioorganic Phosphorus Chemistry and Chemical Biology of Ministry of Education, Tsinghua University, Beijing 100084, China*

Yimeng Zhang − *Department of Chemistry, Beijing Key Laboratory for Analytical Methods and Instrumentation, Kay Lab of Bioorganic Phosphorus Chemistry and Chemical Biology of Ministry of Education, Tsinghua University, Beijing 100084, China*

Hongye Wang − *Department of Chemistry, Beijing Key Laboratory for Analytical Methods and Instrumentation, Kay Lab of Bioorganic Phosphorus Chemistry and Chemical Biology of Ministry of Education, Tsinghua University, Beijing 100084, China*

Complete contact information is available at: https://pubs.acs.org/10.1021/acs.analchem.0c00469

Notes

The authors declare no competing financial interest.

■ ACKNOWLEDGMENTS

This work was financially supported by National Key Research and Development Program of China (No.2016YFA0203101), National Natural Science Foundation of China (nos. 21874080, 21622506, 21621003), and the Taishan Scholar Program of Shandong Province (ts201511027).

■ REFERENCES

(1) Chiu, Y. J.; Cai, W.; Shih, Y. R.; Lian, I.; Lo, Y. H. *Small* **2016**, *12*, 3658−3666.
(2) Jiang, Y.; Shi, M.; Liu, Y.; Wan, S.; Cui, C.; Zhang, L.; Tan, W. *Angew. Chem., Int. Ed.* **2017**, *129*, 11916−11920.
(3) Mathivanan, S.; Ji, H.; Simpson, R. J. *J. Proteomics* **2010**, *73*, 1907−1920.
(4) Valadi, H.; Ekstrom, K.; Bossios, A.; Sjostrand, M.; Lee, J. J.; Lotvall, J. O. *Nat. Cell Biol.* **2007**, *99*, 654−659.
(5) Tian, Y.; Ma, L.; Gong, M.; Su, G.; Zhu, S.; Zhang, W.; Wang, S.; Li, Z.; Chen, C.; Li, L. *ACS Nano* **2018**, *12*, 671−680.
(6) Tiancheng, L.; Mendes, D. E.; Berkman, C. E. *Int. J. Oncol.* **2014**, *44*, 918−922.
(7) Yadav, S.; Boriachek, K.; Islam, N.; Lobb, R.; Möller, A.; Hill, M.; Hossain, S.; Nguyen, N. T.; Shiddiky, M. J. A. *ChemElectroChem* **2017**, *4*, 967−971.
(8) Zhang, D.; Li, W.; Ma, Z. *Biosens. Bioelectron.* **2018**, *109*, 171−176.
(9) Doldán, X.; Fagúndez, P.; Cayota, A.; Laíz, J.; Tosar, J. P. *Anal. Chem.* **2016**, *88*, 10466−10473.
(10) Cao, Y.; Li, L. L.; Han, B.; Wang, Y.; Dai, Y. H.; Zhao, J. *Biosens. Bioelectron.* **2019**, *141*, 11397−11403.
(11) Ye, C.; Zhong, X.; Yuan, R. *Sens. Actuators, B* **2014**, *199*, 101−107.
(12) Forzani, E. S.; Lu, D.; Leright, M. J.; Aguilar, A. D.; Tsow, F.; Iglesias, R. A.; Zhang, Q.; Lu, J.; Li, J.; Tao, N. *J. Am. Chem. Soc.* **2009**, *131*, 1390.
(13) Wang, H.; Yuan, R.; Chai, Y. Q. *Biosens. Bioelectron.* **2013**, *43*, 63−68.
(14) Zhang, H. R.; Wu, M. S.; Xu, J. J.; Chen, H. Y. *Anal. Chem.* **2014**, *86*, 3834−3840.
(15) Qi, H. L.; Zhang, C. X. *Anal. Chem.* **2020**, *92*, 524−534.
(16) Feng, Q. M.; Shen, Y. Z.; Li, M. X.; Zhang, Z. L.; Zhao, W.; Xu, J. J.; Chen, H. Y. *Anal. Chem.* **2016**, *88*, 937−944.
(17) Chen, L.; Zeng, X.; Si, P.; Chen, Y.; Chi, Y.; Kim, D. H.; Chen, G. *Anal. Chem.* **2014**, *86*, 4188−4195.
(18) Zhang, L.; Cheng, Y.; Lei, J.; Liu, Y.; Hao, Q.; Ju, H. *Anal. Chem.* **2013**, *85*, 8001−8007.
(19) Cheng, Y.; Huang, Y.; Lei, J.; Zhang, L.; Ju, H. *Anal. Chem.* **2014**, *86*, 5158−5163.
(20) Chen, Z.; Liu, Y.; Wang, Y.; Zhao, X.; Li, J. *Anal. Chem.* **2013**, *85*, 4431−4438.
(21) Wang, Y.; Li, Z.; Weber, T. J.; Hu, D.; Lin, C. T.; Li, J.; Lin, Y. *Anal. Chem.* **2013**, *85*, 6775−6782.
(22) Zhang, Y. M.; Wang, F.; Zhang, H. X.; Wang, H. Y.; Liu, Y. *Anal. Chem.* **2019**, *91*, 12100−12107.
(23) Fang, D. D.; Zhao, D. D.; Zhang, S. P.; Huang, Y. T.; Dai, H.; Lin, Y. Y. *Sens. Actuators, B* **2020**, *305*, 127544−127552.
(24) Yang, Y.; Jiang, X.; Chao, J.; Song, C. Y.; Liu, B.; Zhu, D.; Sun, Y. Z.; Yang, B. Y.; Zhang, Q. W.; Chen, Y.; Wang, L. H. *Sci. China. Mater.* **2017**, *60*, 1129−1144.
(25) Liu, W.; Liu, Z.; Wang, G.; Sun, X. M.; Li, Y. P.; Liu, J. F. *Sci. China. Mater.* **2017**, *60*, 438−448.
(26) Mathiyazhakan, M.; Upputuri, P. K.; Sivasubramanian, K.; Dhayani, A.; Vemula, P. K.; Zou, P. C.; Pu, K. Y.; Yang, C.; Pramanik, M.; Xu, C. J. *Sci. China. Mater.* **2016**, *59*, 892−900.
(27) Vaz, D. C.; Escudero, E. M.; Cuesta, A. P.; Dapena, F.; Cerrillos, C.; Rueda, M. *Electrochem. Commun.* **2013**, *35*, 61−64.
(28) Jirkovsky, J. S.; Panas, I.; Ahlberg, E.; Halasa, M.; Romani, S.; Schiffrin, D. J. *J. Am. Chem. Soc.* **2011**, *133*, 19432−19441.
(29) Kou, R.; Shao, Y. Y.; Wang, D. H.; Engelhard, M. H.; Kwak, J. H.; Wang, J.; Viswanathan, V. V.; Wang, C. M.; Lin, Y. H.; Wang, Y.; Aksay, I. A.; Liu, J. *Electrochem. Commun.* **2009**, *11*, 954−957.
(30) Steigerwalt, E. S.; Deluga, G. A.; Lukehart, C. M. *J. Phys. Chem. B* **2002**, *106*, 760−766.
(31) Bing, Y. H.; Liu, H. S.; Zhang, L.; Ghosh, D.; Zhang, J. J. *Chem. Soc. Rev.* **2010**, *39*, 2184−2202.
(32) Dey, D.; Bhattacharya, T.; Majumdar, B.; Mandani, S.; Sharma, B.; Sarma, T. K. *Dalton Trans.* **2013**, *42*, 13821−13825.
(33) Naguib, M.; Come, J.; Dyatkin, B.; Presser, V.; Taberna, P. L.; Simon, P.; Barsoum, M. W.; Gogotsi, Y. *Electrochem. Commun.* **2015**, *16*, 61−64.
(34) Ding, L.; Wei, Y. Y.; Wang, Y. J.; Chen, H. B.; Caro, J. G.; Wang, H. H. *Angew. Chem., Int. Ed.* **2017**, *56*, 1−6.
(35) Wang, H. W.; Naguib, M.; Page, K.; Wesolowski, D. J.; Gogotsi, Y. *Chem. Mater.* **2016**, *28*, 349−359.
(36) Ng, V. M. H.; Huang, H.; Zhou, K.; Lee, P. S.; Que, W. X.; Xu, J. Z. C.; Kong, L. B. *J. Mater. Chem. A* **2017**, *5*, 3035−3068.
(37) Naguib, M.; Kurtoglu, M.; Presser, V.; Lu, J.; Niu, J.; Heon, M.; Hultman, L.; Gogotsi, Y.; Barsoum, M. W. *Adv. Mater.* **2011**, *23*, 4248−4253.
(38) Naguib, M.; Mochalin, V. N.; Barsoum, M. W.; Gogotsi, Y. *Adv. Mater.* **2014**, *26*, 992−1005.

(39) Zhang, Z.; Li, H.; Zou, G. D.; Fernandez, C.; Liu, B. Z.; Zhang, Q. R.; Hu, J.; Peng, Q. M. *ACS Sustainable Chem. Eng.* **2016**, *4*, 6763−6771.
(40) Zou, G. D.; Zhang, Z.; Guo, J.; Liu, B. Z.; Zhang, Q. R.; Fernandez, C.; Peng, Q. M. *ACS Appl. Mater. Interfaces* **2016**, *8*, 22280−22286.
(41) Zhang, Q. R.; Teng, J.; Zou, G. D.; Peng, Q. M.; Du, Q.; Jiao, T. F.; Xiang, J. Y. *Nanoscale* **2016**, *8*, 7085−7093.
(42) Chi, C.; Muhammad, B.; Urbankowski, P.; Anasori, B.; Ling, M.; Jiang, J.; Gogotsi, Y. *J. Mater. Chem. A* **2018**, *6*, 4617−4622.
(43) Liu, C.; Guo, J.; Tian, F.; Yang, N.; Yan, F.; Ding, Y.; Wei, J.; Hu, G.; Nie, G.; Sun, J. S. *ACS Nano* **2017**, *11*, 6968−6976.
(44) Zhang, L.; Wang, Y. Z.; Tian, Q. Q.; Liu, Y.; Li, J. H. *Biosens. Bioelectron.* **2017**, *89*, 1013−1019.
(45) Zhang, H. X.; Wang, Z. H.; Zhang, Q. X.; Wang, F.; Liu, Y. *Biosens. Bioelectron.* **2019**, *124*, 184−190.
(46) Wang, J.; Li, W.; Ban, L.; Chen, P.; Du, W.; Feng, X.; Liu, B. F. *ACS Appl. Mater. Interfaces* **2017**, *9*, 27441−27452.

https://dx.doi.org/10.1021/acs.analchem.0c00469
Anal. Chem. 2020, 92, 5546−5553